7 (2): 165-170 (2023)

Journal of Aviation

https://dergipark.org.tr/en/pub/jav

e-ISSN 2587-1676

Production of Nanostructured Fasteners with High Shear and Fatigue Strength for Using in Aircraft Components

Kazım Buğra Gürbüz [1], Mustafa Taşkın[2*]

[1] Mersin University, Metallurgical and Material Engineering Department, Mersin, Türkiye. (bugragurbuz89@gmail.com)
[2*] Mersin University, Metallurgical and Material Engineering Department, Mersin, Türkiye. (taskinmustafa33@gmail.com)

Article Info

Received: 29 November 2022
Revised: 11April 2023
Accepted: 11 May 2023
Published Online: 22 June 2023

Keywords:
HSLA Steels
Microalloyed
Heat treatment cyclic
Multi-axial forging
Aircraft

Corresponding Author: *Mustafa Taşkın*

RESEARCH ARTICLE

https://doi.org/10.30518/jav.1211562

Abstract

Multi-axis forging (MAF) and cyclic heat treatment are among the most widely used and easy to apply grain refinement methods. In this study, micro-alloyed steel samples were first subjected to MAF treatments at 880° C. Microstructural analysis showed that the average grain size, which was 13.2 µm initially, decreased to 11.2 µm application of the MAF. As a second-grain refinement technique, cyclic heat treatment was used. Samples were subjected to 1, 3, 5, 7, and 10 cyclic quenching. With this method, it was observed that the average grain size decreased to 2,3 µm. The mechanical tests showed that the second MAF process increased the yield and tensile strength of the material by about 16% while decreasing the elongation by %2. These tests also presented cyclic quenching increased tensile strength of the samples after the first application.

1. Introduction

Microalloyed steels or often referred as high strength low alloy (HSLA) steels, are subgroup of low carbon steel that typically contain less than 0,2% carbon, up to 2% manganese, and a small amount of other alloying elements, such as niobium, vanadium, titanium, molybdenum, aluminum (Baker, 2016; Shao et al., 2018). Generally, these steels contain a combination of these alloying elements up to 2%wt in weight to reach yield strength greater than 275 MPa. In many industries such as automotive, aerospace, pipelines, construction, railway, nuclear power plants, and naval industry, micro-alloyed steels are widely used as a structural material due to its remarkable mechanical properties, formability, lightweight and good weldability (Shao et al., 2018; Vervynckt et al., 2012; Shi et al., 2019; Ledermueller, et al., 2020; Ramesh, et al., 2020; Li et al., 2020).

Although each alloying element has different characteristics that alter mechanical properties, the primary purpose of microalloying addition is to obtain ferrite strengthening via solid solution strengthening, precipitation hardening and, most importantly, grain refinement (Vervynckt et al., 2012). Many studies have shown that niobium is one of the most effective alloying elements used to strengthen micro-alloyed steels, by not only retarding recrystallization and growth of ferrite grains but also contribute solid solution strengthening by precipitate into ferrite in the form of Nb (C, N) (Cao et al., 2007; Chen et al., 2013). Vanadium, on the other hand, is almost entirely soluble in the austenite phase and contributes to the increase in strength by precipitation in the form of V (C, N) during the austenite ferrite transformation (Baker, 2009; Dewi et al., 2020; Lagneborg et al., 1999; Singh et al., 2020). Studies show that titanium is used for the precipitation hardening mechanism and sulphide shape control instead of grain refinement. Although its contribution to precipitation hardening is much more effective than vanadium or niobium, the grain refinement effect is weaker than theirs. Therefore, titanium is often combined with vanadium and niobium for better results (Baker, 2019). Apart from these most commonly used elements, the addition of aluminum usually provides deoxidation of the steel but also prevents grain growth in the Al (N) form (Vervynckt et al., 2012).

Despite the fact that the alloy composition has a specific effect on mechanical properties, the distinctive properties of micro-alloyed steels are mainly determined by the heat treatment, severe plastic deformation and/or thermomechanical processes applied after casting (Majta et al., 2007). There are multiple reasons to use these processes, such as solid solution strengthening and precipitation hardening, but in general superior mechanical properties of micro-alloyed steels rely on grain refinement. Combining the proper chemical composition and process parameters makes obtaining different microstructures, grain sizes, and desired properties possible. Studies show that cyclic heat treatment is more effective than conventional heat treatments to optimize strength, ductility, and toughness (Ray et al., 2003; Wang, et

al., 2007). The primary purpose of the cyclic processes is to reduce the austenite grain size in each cycle to ensure that the final grain size is as fine as possible. Since the grain reduction effect of these treatments depends on controlling the austenite phase, these processes are insufficient in most steels where only austenitic growth can be prevented by operating temperature and waiting time. As for HSLA steels, austenite growth is mainly controlled by micro-alloy elements; therefore, thermal cycles are more effective for these materials. These steels are also known as "Micro-alloyed Steels" due to the small amount of alloying elements they contain. These steels have superior mechanical properties and often better corrosion resistance than rolled carbon steels. Thanks to these properties, HSLA steels are preferred in many fields, especially in the aviation and space sectors (Davis et al., 2001).

Like heat treatment, severe plastic deformation (SPD) techniques focus on grain refinement to increase the mechanical properties of the micro-alloyed steels. In this technique, grain refinement is achieved by imposing large accumulated plastic strains on the material at room or elevated temperatures (Song et al., 2006). There are many SPD methods, such as equal-channel angular pressing (ECAP), accumulative roll bonding (ARB), high-pressure torsion (HPT), and multi-axial forging (MAF), have been successfully applied to grain refinement (Song et al., 2006; Nakao et al., 2011). Among these techniques, MAF stands out because it is relatively simple, easily adaptable for different materials and geometries and can be used to produce large bulk materials (Xia et al., 2013). The material is subjected to high-pressing forces on different axes in the austenite region in the MAF method. The size and orientation homogeneity of the grains is achieved by rotating the materials 90 ° around their axis at the end of each loading. In this process, slip shear created by the axial loading produces deformed bands in deformed grains in a certain direction. When the order of the load is changed, new deformation bands are formed in different directions from the first bands. The intersection of these bands causes the formation of many sub-particles in the material. As the angles of these sub-grains increase in the continuation of the process, the sub-grains turn into excellent average grains (Huang et al., 2006).

The main purpose of this paper is to determine the appropriate thermal conversion and multi-axial forging parameters that can be used to obtain ultrafine grain in micro-alloyed steels. For this purpose, samples with the same chemical composition were subjected to mechanical and microstructural tests after being subjected to different thermal cycling and multi-axial forging processes.

2. Materials and Methods

2.1. Preparation of the sample

The micro-alloyed steel, whose composition (by ARL Model 4460 Thermo Scientific spectrometer) is listed in Table 1, was chosen in this study. The chemical composition was investigated according to ASTM E45.

First, the micro-alloyed steel was melted in the induction furnace at 1200 °C. After the preparation of the alloy, the melt was poured into the resin molds, and the physical cleaning of the sample surfaces after solidification.

Table 1. Chemical composition of the produced samples (wt%)

C	Mn	V	Ti	Al	Nb	Mo	Ni	Cr	Cu	Si	P	S
0.138	1.468	0.066	0.010	0.017	0.040	0.174	0.049	0.092	0.098	0.363	0.012	0.016

The samples were subjected to multi-axial forging and cyclic quenching for fine grain size. The samples were first subjected to Multi-Axial Forging (MAF) in a hydraulic press to achieve this. The schematic representation of the forging process is given in Figure 1.

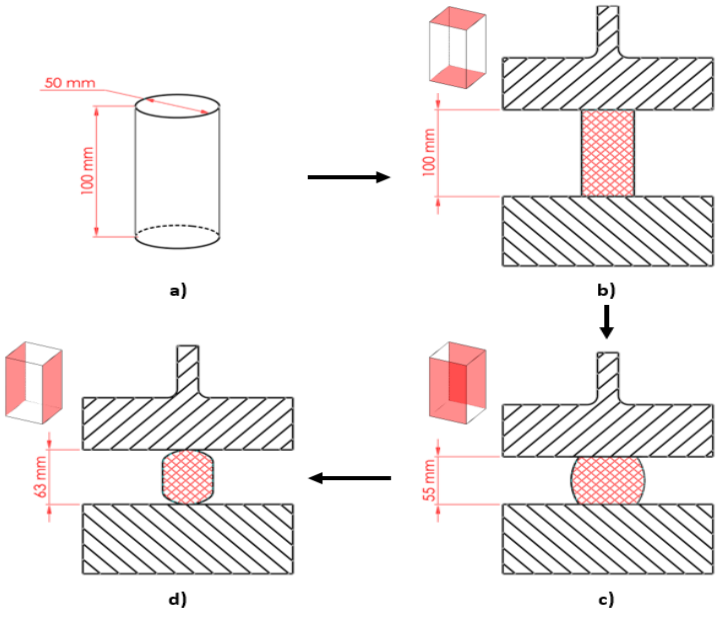

Figure 1. Schematic forging steps: **a)** initial dimensions of the samples, **b)** – **d)** forging in different axes.

A sample was marked as "No.0" and selected as a reference sample. The remaining samples were heated to 880°C and held at this temperature for 60 min to obtain the austenite phase. After the phase transformation, the samples were forged (Figure.1. b – d), with 20% constant strain in all three axes. The samples were directly quenched at the water at room temperature right after the forging was completed. Samples took the form of a slightly curved rectangular prism after forging. The average length and width of the samples were measured as 88 mm by 52 mm, respectively.

When the multi-axial forging was completed, specimens were subjected to cyclic quenching to apply additional grain size reduction. The main purpose of this process is to reduce the final grain size of the materials by repeated austenite → martensite transformation from the α + γ region. Cyclic heat treatment was applied to samples 1, 3, 5, 7, and 10 times, and they were marked as "A.2", "A.3", "A.4", "A.5" and "A.6" respectively. The number of heat treatment cycles and total strain applied to the samples and processing route of the cyclic quenching used on the samples is given in Table 2 and Figure 2. respectively.

Table 2. Strain rate and number of the cyclic quenching repeats applied to samples

Sample Code	Total Strain (All Axes) (%)	Cyclic Quenching Repetitions (Times)
No.0.	0	0
A.1.	20	0
A.2.	20	1
A.3.	20	3
A.4.	20	5
A.5.	20	7
A.6	20	10

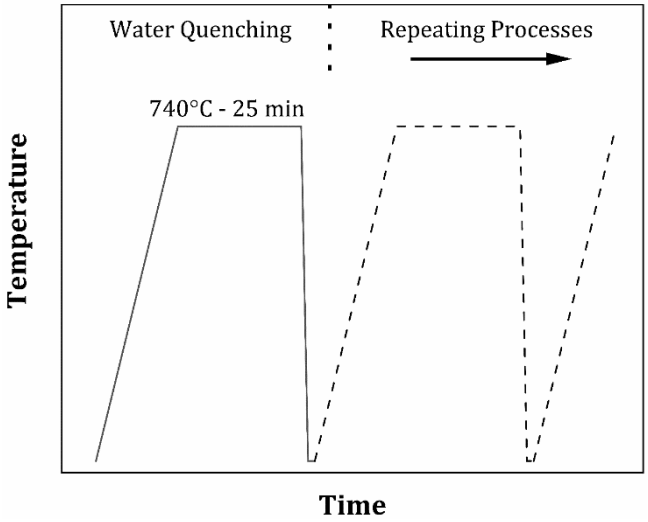

Figure 2. Cyclic quenching process route applied on the samples

As shown in Figure 2., to transform the α phase into the α + γ phase, the samples were heated to 740° C and kept at this temperature for 25 minutes to achieve sufficient transformation. After the transformation, the samples were quenched in water at 23° C to obtain martensite from the transformed γ phase. The number of repetitions applied to the samples was determined according to the numbers indicated in Table 2.

2.2. Microstructure observation

Optical microscopy and scanning electron microscopy (SEM) were performed to determine the effect of the applied processes on the average grain size of the specimens. The samples were first cut in appropriate sizes using a Metkon brand Metacut 251 model oil-cooled cutting disc to examine the microstructure in the optical microscope. After sectioning, samples were hot mounted by Tronic brand EcoPress 30 model hot bakelite molding device. The grinding process was applied to each sample under water using sandpaper with SiC particles 80, 120, 240, 600, 800, and 1200 grit sizes, respectively. After the process was completed, the samples were taken to the rough polishing process. Rough polishing was done using 9 µm and 6 µm Metkon Diapat-M branded diamond suspensions on discs covered with plain fabric cloth, respectively. After rough polishing, 3 µm and 1 µm Metkon Diapat-M branded diamond suspensions were used, respectively, on the discs covered with velvet fabric for precision polishing. Sanding and polishing processes were carried out using the automatic polishing device (Struers RotoPol-21).

After polishing, the samples were washed with distilled water and alcohol, then dried under warm air. Finally, the samples were etched to reveal the grain boundaries under an optical microscope. Etching was carried out by keeping the sample surfaces in a 4% nital solution at room temperature for 4 minutes. The microstructures were observed by inverted type microscope (Zeiss, Axio).

2.3. Mechanical tests

For the tensile test, the samples were prepared according to the DIN 50125: 2016-2 B tensile test standard for metallic materials. This standard obtained a bone-type test specimen of 8 mm diameter and 51 mm length. Three tensile test pieces were prepared in each sample with selected dimensions to perform the tensile test properly and avoid a possible error. The machined parts were tested on tensile tester (Zwick, Roell Z250, 250kN capacity). All tensile tests were carried out at standard 24 ° C and a 0.5 mm/sec speed. The test results were transferred to the computer environment with the TestXper III program, and the raw data required for drawing the stress-strain graph was obtained. The test pieces' elastic modulus, elongation, yield, and tensile strength were calculated using the same program.

A digital hardness tester (Galileo, ErgoTest Digi 25R), was used for the hardness measurements of samples. Five measurements were made at equal intervals along a line passing through the center of each sample to measure the hardness accurately. The hardness values of the samples were calculated by disregarding the largest and the smallest value from the results obtained and finding the average of the remaining three measurement points.

3. Result and Discussion

3.1. Microstructural Examination

To determine the effect of cyclic quenching, microstructure analysis, tensile and hardness tests were applied to the samples.

The microstructure image was taken at 200x magnification of the part marked with No.0., which belongs to the grain reduction processes applied to the samples, is given in Figure 3.

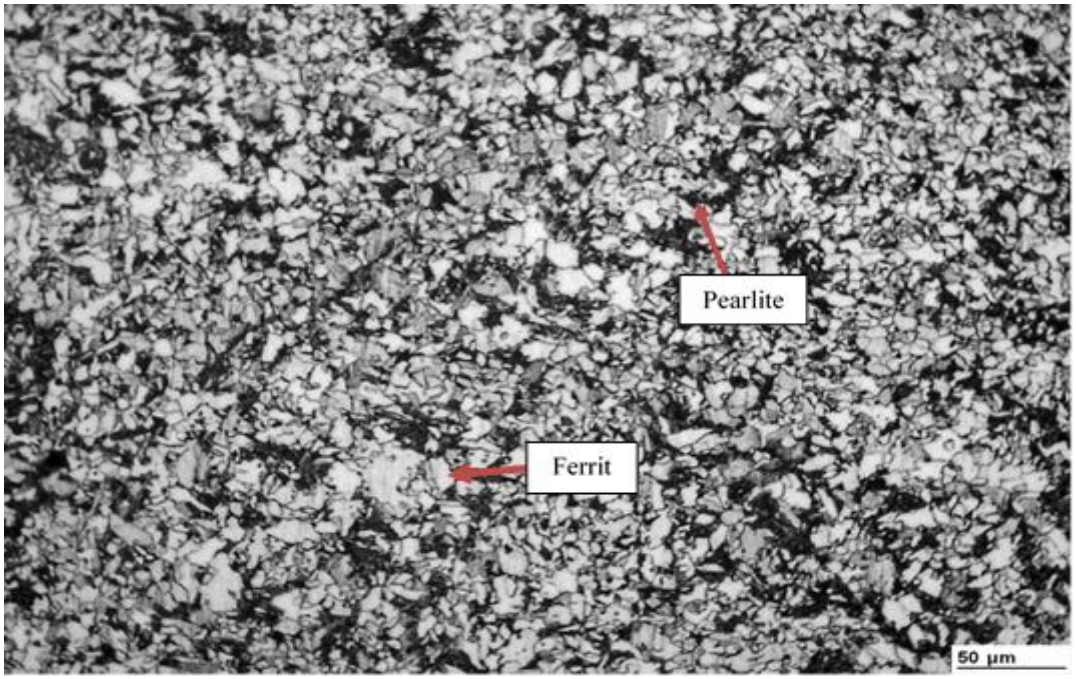

Figure 3. Optical microstructure of sample No.0

In the first examination of the microstructure seen in Figure 3, it is clearly seen that the material structure is formed of ferrite (light-colored islets) + perlite (dark areas). The average grain size of the No.0. sample was determined as 13.3 µm.

The microstructure of the samples that were subjected to the MAF process and cyclic heat treatment was given in Figure 4.

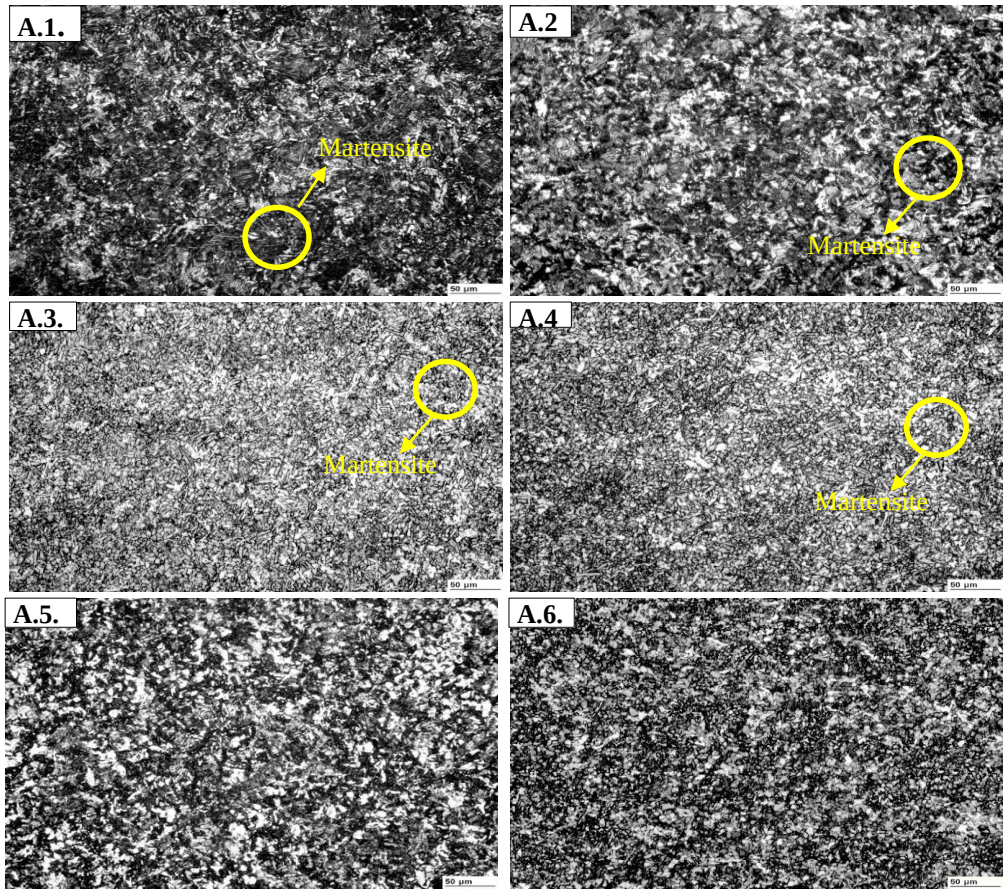

Figure 4. Optical microstructures of the samples

From Figure 4, it can be observed that the grain size decreases with each thermal cycle. When the images are examined separately, it is seen that lamellar martensite formation has started in the A.1. sample in addition to the refining of perlite and ferrite phases in No.0. sample. The average grain sizes of the samples calculated by computer are shown in Table 3 and Figure 5. In the material's austenite region, the martensite phase (lamellar structures) formed in addition to ferrite and pearlite is observed in the microstructure after forging in three axes. At the same time, the grain reduction effect of the amount of strain applied to the material is seen.

Table 3. Average grain size of the group "A" samples

Sample Code	Cyclic Quenching Repetitions (Times)	Average Grain Size (µm)
A.1.	0	11.2
A.2.	1	9.2
A.3.	3	8.7
A.4.	5	7.6
A.5.	7	5.86
A.6.	10	2.3

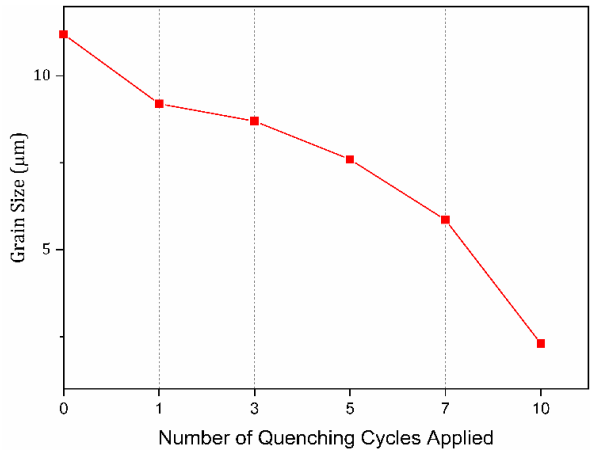

Figure 5. Average grain size of the samples

As shown in Table 3 and Figure 5, average grain size reduces with increasing thermal cycles as expected. The initial quenching resulted in an approximately 18% reduction in the average grain size of the material. In addition, it was calculated that cyclic quenching decreased the average grain size of the samples by 22% in 3 repetitions, 32% in 5 repetitions, 48% in 7 repetitions, and finally %79 in 10 repetitions.

3.2. Tensile Test

The tensile tests were performed under standard laboratory conditions at 0.5 mm/min loading velocity. Numerical data of the tensile test and the stress-strain curves of these data are given in Tables 5 and Figure 6, respectively.

Table 5. Tensile test result of the samples

Sample Code	Elongation (%)	Yield Strength (MPa)	Tensile Strength (MPa)
A.1.	17	512	794
A.2.	29.2	490.3	580.5
A.3.	28.6	438	584
A.4.	28	431	608
A.5.	27.6	460.8	609.5
A.6.	27	389	635

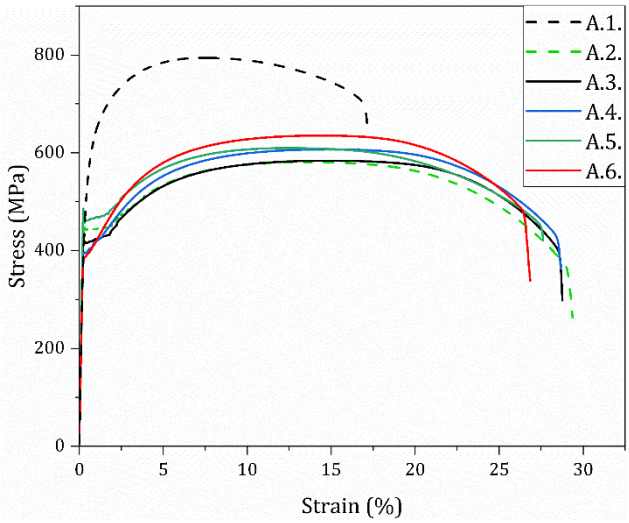

Figure 6. Stress – strain curve of samples.

When the strain-strain curve shown in Figure 6 is examined, it is seen that the A.1. sample without heat treatment has the highest yield and tensile strength and the lowest percentage elongation compared to the other samples. It is easily seen from Table 5 that after the initial quenching, the increasing number of quenching cycles increases the tensile strength while decreasing the elongation by a very small amount. Furthermore, it was found that the applied quenching cycles caused almost no change in the toughness of the materials.

3.3. Hardness Test

Hardness tests of all samples were done using the Brinell scale. Figure 7 shows the hardness values versus the number of thermal cycles of the samples.

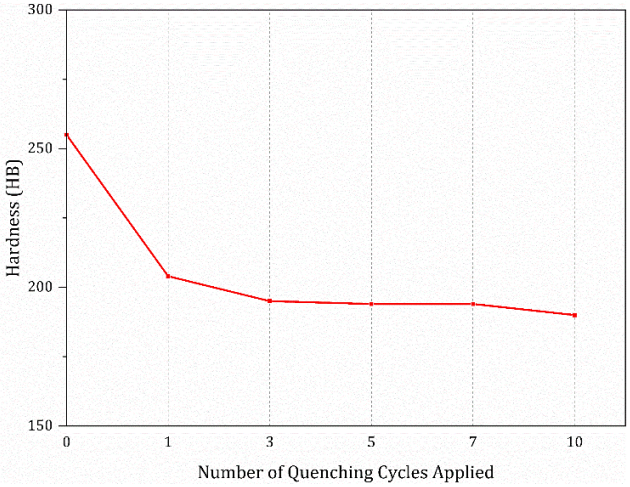

Figure 7. Hardness values of the samples

It can be seen in Figure 7 that the first heat treatment significantly reduced the hardness value of the material. On the other hand, seen that the increasing number of thermal cycles has almost no effect on the hardness values of the materials.

4. Conclusion

This study investigated the effect of cyclic heat treatment on micro-alloyed steels. The observations are summarized in the following part;

- As a result of the first MAF process, it was observed that there was an approximately 16% reduction in grain size.
- Each quenching cycle resulted in a reduction in the grain size of the samples, as expected.
- After the 10th quenching, the average grain size of the sample was measured as 2,3 µm. This shows that an approximately 83% reduction is achieved with ten quenching cycles.
- Although a decrease in tensile strength was observed after the first quenching process, a specific increase was observed with increasing cycles.
- Even though the elongation increased by approximately 72% after the first quenching process, no significant change was observed in the ongoing quenching cycles.
- Like elongation, initial quenching significantly lowered the hardness of the sample, but increasing the number of cycles was found to have no significant effect on hardness.
- It has been observed that increasing the quenching cycle decreases yield strength while increasing tensile strength. This situation can be interpreted that the quenching cycle causing an increase in plastic-forming capability in the samples.

Ethical approval

Not applicable.

Conflicts of Interest

The authors declare that there is no conflict of interest regarding the publication of this paper.

Acknowledgement

This study was supported by Mersin KOSGEB Directorate.

References

Baker, T.N. (2009). Processes, microstructure and properties of vanadium microalloyed steels. Materials Science and Technology, 25(9), 1083-1107.

Baker, T.N. (2016). Microalloyed steels. Ironmaking & Steelmaking, 43(4), 264-307.

Baker, T.N. (2019), Titanium microalloyed steels. Ironmaking & Steelmaking, 46(1), 1-55.

Cao, J.-c., et al. (2007). Effect of Niobium on Isothermal Transformation of Austenite to Ferrite in HSLA Low-Carbon Steel. Journal of Iron and Steel Research, International, 14(3), 52-56.

Chen, Y., et al. (2013). Effect of dissolution and precipitation of Nb on the formation of acicular ferrite/bainite ferrite in low-carbon HSLA steels. Materials Characterization, 84, 232-239.

Davis, J. R., Alloying (2001). Understanding the Basics. ASM International: Materials Park, 193-209.

Dewi, H.S., Volpp J., & Kaplan A.F.H. (2020). Short thermal cycle treatment with laser of vanadium microalloyed steels. Journal of Manufacturing Processes, 57, 543-551.

Huang, J. and Z. Xu (2006). Evolution mechanism of grain refinement based on dynamic recrystallization in multiaxially forged austenite. Materials Letters, 60(15), 1854-1858.

Lagneborg, R., et al. (1999). Role of vanadium in microalloyed steels. Scandinavian Journal of Metallurgy, 28,186-241.

Ledermueller, C., et al. (2020). Microalloying effects of Mo versus Cr in HSLA steels with ultrafine-grained ferrite microstructures. Materials & Design, 185, 108278.

Li, X., et al. (2020). Acquiring a low yield ratio well synchronized with enhanced strength of HSLA pipeline steels through adjusting multiple-phase microstructures. Materials Science and Engineering: A, 785, 139350.

Majta, J. & Muszka K. (2007). Mechanical properties of ultra fine-grained HSLA and Ti-IF steels. Materials Science and Engineering: A, 464(1): p. 186-191.

Nakao, Y. & Miura H. (2011). Nano-grain evolution in austenitic stainless steel during multi-directional forging. Materials Science and Engineering: A, 528(3), 1310-1317.

Ramesh, R., et al. (2020). Microstructural characterization and tensile behavior of Nd:YAG laser beam welded thin high strength low alloy steel sheets. Materials Science and Engineering: A,780,139178.

Ray, P.K., Ganguly R.I., & Panda A.K. (2003). Optimization of mechanical properties of an HSLA-100 steel through control of heat treatment variables. Materials Science and Engineering: A, 346(1), 122-131.

Shao, Y., et al. (2018). Formation mechanism and control methods of acicular ferrite in HSLA steels: A review. Journal of Materials Science & Technology, 34(5), 737-744.

Shi, R., et al. (2019). Microstructure evolution of in-situ nanoparticles and its comprehensive effect on high strength steel. Journal of Materials Science & Technology, 35(9), 1940-1950.

Singh, A.P. & Pant, G. (2020). Mechanical behaviour of vanadium microalloyed steel under control environment compression. Materials Today: Proceedings, 26, 2525-2527.

Song, R., et al. (2006). Overview of processing, microstructure and mechanical properties of ultrafine grained bcc steels. Materials Science and Engineering: A, 441(1), 1-17.

Vervynckt, S., et al. (2012). Modern HSLA steels and role of non-recrystallisation temperature. International Materials Reviews, 57(4), 187-207.

Wang, Q.F., et al. (2007). Refinement of Steel Austenite Grain Under an Extremely High Degree of Superheating. Journal of Iron and Steel Research, International, 14(5), 161-166.

Xia, X.-s., et al. (2013). Microstructure and mechanical properties of isothermal multi-axial forging formed AZ61 Mg alloy. Transactions of Nonferrous Metals Society of China, 23(11), 3186-3192.

Cite this article: Gurbuz, K.B, Taskin, M. (2023). Production of Nanostructured Fasteners with High Shear and Fatigue Strength for Using in Aircraft Components. Journal of Aviation, 7(2), 165-170.